

# Can Single-Atom Change Affect Electron Transport Properties of Molecular Nanostructures such as C<sub>60</sub> Fullerene?

Xiaoliang Zhong and Ravindra Pandey\*

Department of Physics, Michigan Technological University, Houghton, Michigan 49931

Alexandre Reily Rocha

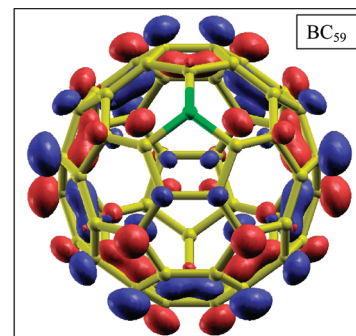
Centro de Ciências Naturais e Humanas, Universidade Federal do ABC, Santo André, Brazil

Shashi P. Karna\*

US Army Research Laboratory, Weapons and Materials Research Directorate, ATTN: RDRL-WM, Aberdeen Proving Ground, Maryland 21005-5069

**ABSTRACT** At the nanoscale, even a single atom change in the structure can noticeably alter the properties, and therefore, the application space of materials. We examine this critical behavior of nanomaterials using fullerene as a model structure by a first-principles density functional theory method coupled with nonequilibrium Green's function formalism. Two different configurations, namely, (i) endohedral (B@C<sub>60</sub> and N@C<sub>60</sub>), in which the doping atom is encapsulated inside the fullerene cage, and (ii) substitutional (BC<sub>59</sub> and NC<sub>59</sub>), in which the doping atom replaces a C atom on the fullerene cage, are considered. The calculated results reveal that the conductivity for the doped fullerene is higher than that of the pristine fullerene. In the low-bias regime, the current (I) voltage (V) characteristic of the endohedral as well as the substitutional configurations are very similar. However, as the external bias increases beyond 1.0 V, the substitutional BC<sub>59</sub> fullerene exhibits a considerably higher magnitude of current than all other species considered, thus suggesting that it can be an effective semiconductor in *p*-type devices.

**SECTION** Nanoparticles and Nanostructures



Electronic structure of BC<sub>59</sub> (C in yellow and B in green)

Molecular nanoscale electronic devices have attracted a great deal of attention in recent years.<sup>1</sup> Experimental and theoretical studies aimed at understanding the underlying physics of molecular and nano-electronic devices<sup>2,3</sup> have begun to shed light on electron transport mechanisms through molecules and engineered nanomaterials and help identify appropriate molecular and nanoscale architectures for effective functional elements in electronic devices. Among others, carbon fullerene is one of the most stable and well-known nanoscale molecular structures. Furthermore, its structure and electron transport properties have been the subject of extensive studies for its potential applications as spin valves<sup>4,5</sup> and electro-mechanical amplifiers<sup>6</sup> to name just a few. Carbon fullerenes are composed of a sheet of linked hexagonal rings separated by pentagonal (sometimes heptagonal) rings that help curve the structure into a spherical empty cage. By far the most common one is the Buckminster fullerene, C<sub>60</sub>, discovered accidentally at Rice University in the late 1980s.<sup>7</sup> It has a high symmetry of icosahedra, I<sub>h</sub>, in which all the C atoms are

equivalent with sp<sup>2</sup> hybridization. C<sub>60</sub>, however, does not exhibit “superaromaticity”, i.e., the electrons in the hexagonal rings do not delocalize over the molecule. Therefore C<sub>60</sub> often acts as a semiconductor quantum dot with an energy gap of about 1.5 eV.<sup>8</sup> Since C<sub>60</sub> is a true nanoscale single molecule, its electronic structure and energy levels can be considerably affected by modifying a single atom in its structure. Thus, doping of fullerenes can be generally expected to change their electronic conductivity due to modification in the density of states near the Fermi surface. Indeed, a recent experimental study<sup>9</sup> has shown that the NC<sub>59</sub> molecule acts as a molecular rectifier in a double barrier tunnel junction via the single electron tunneling effect.

Following the semiconductor analogy, one may find that B and N atoms substituting C atoms in the fullerene cage can act as an “acceptor” and a “donor”, respectively, thus modifying

**Received Date:** March 18, 2010

**Accepted Date:** April 27, 2010

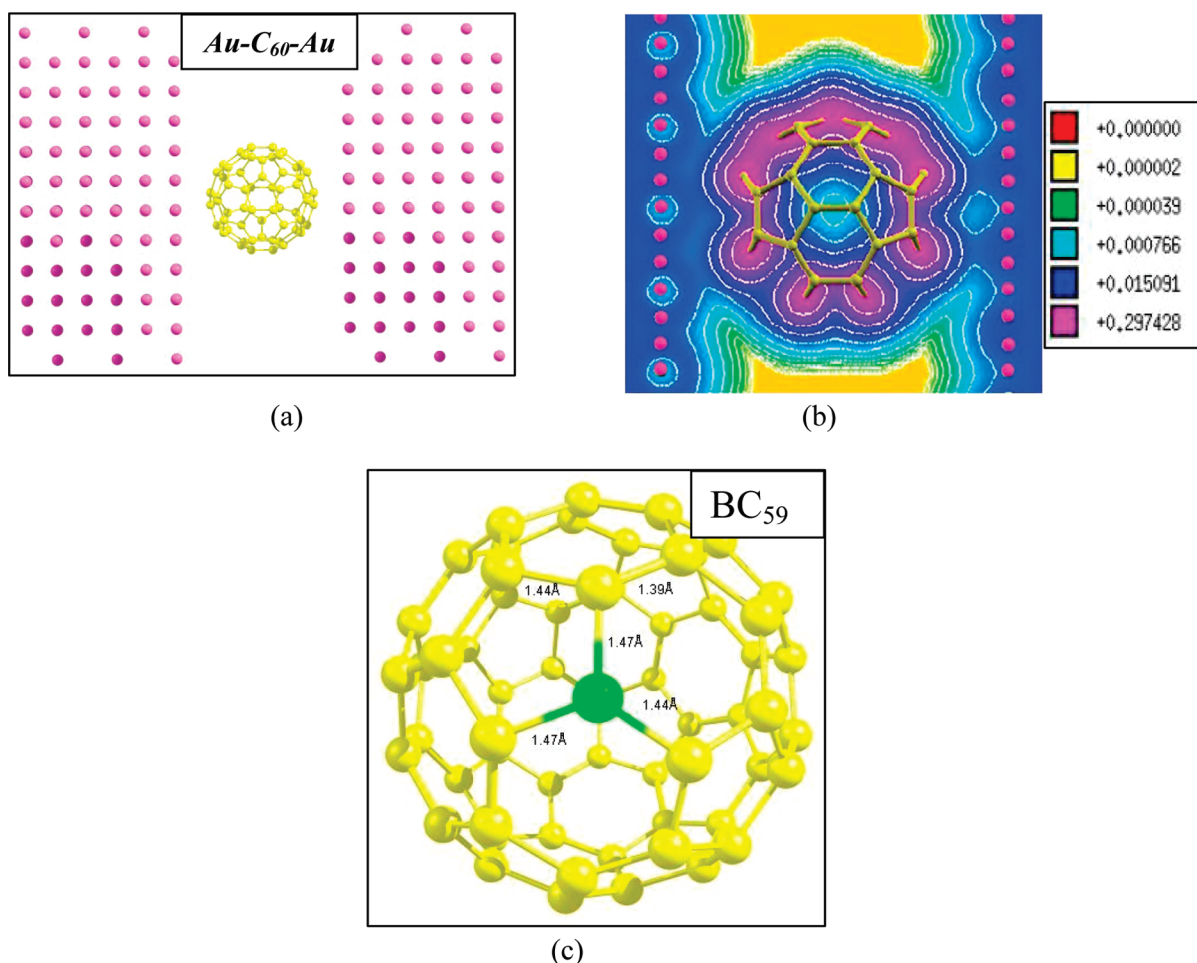


**Figure 1.** (a) A schematic illustration of the Au–C<sub>60</sub>–Au system. (b) A charge density contour plot of the Au–C<sub>60</sub>–Au system, in units of electrons/bohr.<sup>5</sup> (c) The structural configuration of BC<sub>59</sub>. Atomic symbols: Au in magenta, C in yellow, and B in green.

its electron transport properties similar to those in Si. In order to realize such *p*- and *n*-type doped fullerenes, there have been several attempts in the recent years to synthesize BC<sub>59</sub><sup>10</sup> and NC<sub>59</sub>.<sup>11</sup> These experimental efforts have been complemented by several theoretical studies focused mainly on the calculations of the stability and electronic properties of BC<sub>59</sub><sup>12</sup> and NC<sub>59</sub>.<sup>13,14</sup>

While BC<sub>59</sub> and NC<sub>59</sub> offer a substitutional approach to modifying electronic structure of fullerene for electronic device applications, endohedral fullerenes encapsulating atoms or molecules inside the fullerene cage provide an alternative and additional approach to altering the electronic properties of fullerenes, not available in bulk semiconductors or any other materials. Generally, noble gas<sup>15</sup> or metal<sup>16</sup> endofullerenes have been characterized. A few studies have also focused on N-encapsulated endofullerene. These studies suggest that molecular nitrogen can be considered as a van der Waals molecule trapped inside the fullerene cage.<sup>17</sup> Surprisingly, B-encapsulated endofullerenes have not yet been investigated, although encapsulation of a smaller boron atom inside the cage can be expected to form a stable B@C<sub>60</sub> endofullerene.

In this paper, we consider B- and N-doped fullerenes, namely, the B@C<sub>60</sub> and N@C<sub>60</sub> endofullerenes and the

substitutional derivatives, BC<sub>59</sub>, and NC<sub>59</sub>, where the dopant atom has replaced one carbon atom on the cage. The aim of the present study is twofold: (i) to understand the effect of a single-atom change in nanoscale structure on electronic structure and electron transport and (ii) to determine the effect of the chemical nature (B vs N) as well as the geometrical position (i.e., substitutional vs interstitial) of the dopant on current–voltage (i.e., I–V) characteristics of fullerenes.

The electron transport calculations were performed with the use of density functional theory<sup>26–28</sup> (DFT) together with the nonequilibrium Green's function (NEGF) method.<sup>29,30</sup> A schematic illustration of the central scattering region of the model architecture is shown in Figure 1.

There are two C–C bond lengths (*R*<sub>C–C</sub>) in the optimized fullerene configuration: 1.45 Å for pentagons (type I) and 1.40 Å for hexagons (type II), which compare well with the previously calculated values of 1.45 and 1.37 Å, respectively.<sup>18</sup> Similarly, the calculated gap of about 1.3 eV between the highest occupied molecular orbital (HOMO) and the lowest unoccupied molecular orbital (LUMO) is in agreement with the previous studies.<sup>19</sup>

In the endofullerenes (B@C<sub>60</sub> and N@C<sub>60</sub>), both B and N atoms occupy the center of the fullerene cage, with bond

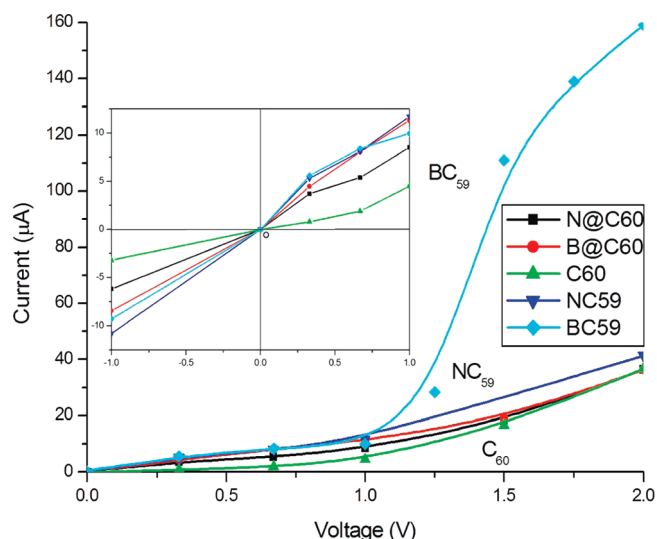


**Figure 2.** The current–voltage characteristic of  $C_{60}$ ,  $BC_{59}$ ,  $NC_{59}$ ,  $B@C_{60}$ , and  $N@C_{60}$ .

lengths,  $R_{B-C}$  or  $R_{N-C}$ , of 3.58 Å. There appears to be no distortion in the surrounding cage due to the atomic dopants. For the substitutional fullerenes,  $BC_{59}$  and  $NC_{59}$ , the overall distortion in the cage induced by the substituted dopants is found to be small in agreement with previous studies.<sup>14</sup> The structural distortion in the substitutional derivatives is also reflected in the electronic polarization; the calculated value of the dipole moment is 0.71 and 1.62 debye for  $BC_{59}$  and  $NC_{59}$ , respectively.

We begin with a pristine  $C_{60}$  molecule to benchmark our results, since its electronic transport properties have been studied extensively.<sup>20–22</sup> An inspection of the calculated current ( $I$ )–voltage ( $V$ ) characteristics of  $C_{60}$ , shown in Figure 2 suggests a metal-like conduction in the low bias range of  $-1$  to  $+1$  V. With the increase in the external bias to 2 V, a significant increase in current occurs. This can be interpreted in terms of the transmission function, which characterizes the intrinsic transport characteristics of the system.

The transmission function as a function of the applied bias and the density of states for the  $C_{60}$  molecule is shown in Figure 3. In general, every transmission peak in the bias window corresponds to a certain molecular orbital (MO), including the intrinsic orbitals of the molecule and the hybridized orbitals of the molecule with the gold leads. For  $Au-C_{60}-Au$ , a large HOMO–LUMO gap reflects itself in a vanishing transmission near the Fermi region. The closest transmission peak at  $-0.8$  eV is due to the HOMO-derived states, whereas the peak at  $\sim 0.8$  eV is due to the LUMO-derived states (Figure 3) resulting in significantly higher currents at the higher bias relative to those at lower ones. Note that the bias-induced shift of the MOs results in a shift of transmission peaks, as shown in Figure 3. These results are consistent with previously reported theoretical studies on  $C_{60}$ .<sup>21,22</sup>

Figure 2 also show the  $I$ – $V$  characteristics of B- and N-doped fullerenes, where substantial device conduction was predicted for  $BC_{59}$  at higher bias. Specifically, the current

rises at a much faster rate for  $BC_{59}$ . Also, the magnitude of the current ( $I$ ) for  $BC_{59}$  at higher bias voltage, (e.g., 2 V), is significantly higher than those in other fullerenes (Figure 2). In the low-bias range ( $< 1$  V), the current remains nearly the same in the pristine and doped fullerenes (Figure 2). It appears that the role of the substitutional B is significantly different from either substitutional N or encapsulated B and N in the cage in determining the electronic transport properties of the doped fullerenes.

Analysis of MOs indicates that the atomic dopants at the endohedral site in the cage contribute to the formation of HOMOs and LUMOs in  $B@C_{60}$  and  $N@C_{60}$ . There exist interband states induced by B and N in the vicinity of the Fermi level (as also seen in the calculated density of states—not shown here). Boron appears to couple with contact Au atoms, whereas nitrogen couples with the C atoms in the cage to form the states near the Fermi energy. We note that the charge transfer between the endohedral dopants (B, N) and the fullerene cage is found to be negligibly small.

For  $BC_{59}$ , an examination of the transmission functions (Figure 3) reveals the appearance of diffusive transmission peaks near the Fermi region. This is further confirmed by the calculated density of states (see Supporting Information). Interestingly, the MOs near the HOMO of  $BC_{59}$  and  $NC_{59}$  are dominated by the contact Au orbitals. Moreover, the peak at  $-0.6$  eV for  $BC_{59}$  is rather delocalized within the gold contact, leading to a very diffusive transmission without showing a distinguishable peak. One can then conclude that the coupling of the Au contact and  $BC_{59}$  opens the electron transport channels due to the delocalized Au–B hybrid states, resulting in rather high currents for the case of substitutional B relative to the case of substitutional N in the fullerene cage. A stronger tendency of boron MOs to hybridize with Au orbitals has been shown to be due to the electron deficient nature of B in our previous studies on the electronic transport of boron nanostructures.<sup>23</sup>

It is tempting to interpret the calculated results of the effect of the B and N substitutions on the  $I$ – $V$  characteristics of fullerene in terms of the bulk semiconductor physics. The considerably larger magnitude of the current for  $BC_{59}$  relative to  $NC_{59}$  at higher bias voltages suggests that the doped fullerene molecule shows a better “hole” conduction than “electron” conduction. Although, the present study focuses on the calculations of current due to “electron transport”, the ease of “hole” conduction over electron conduction in doped fullerene can be also understood from the electronic structure and electron transport of the pristine fullerene. The electrons in the hexagonal carbon rings are known to be highly localized and do not lend themselves easily to participate in electron transport. Thus the fullerene molecule does not offer sufficient electron charge carriers for transport. Any additional electron, for example the one available from the substitution of a C atom by N, thus acts as an electron trapped on a semiconductor quantum dot, yielding nonvanishing—albeit small—current. Substitution by an electron deficient atom, such as B, which creates a hole in fullerene structure, attracts electrons from the adjoining carbon atoms as well as the metal electrodes in the bonding region, which in turn move

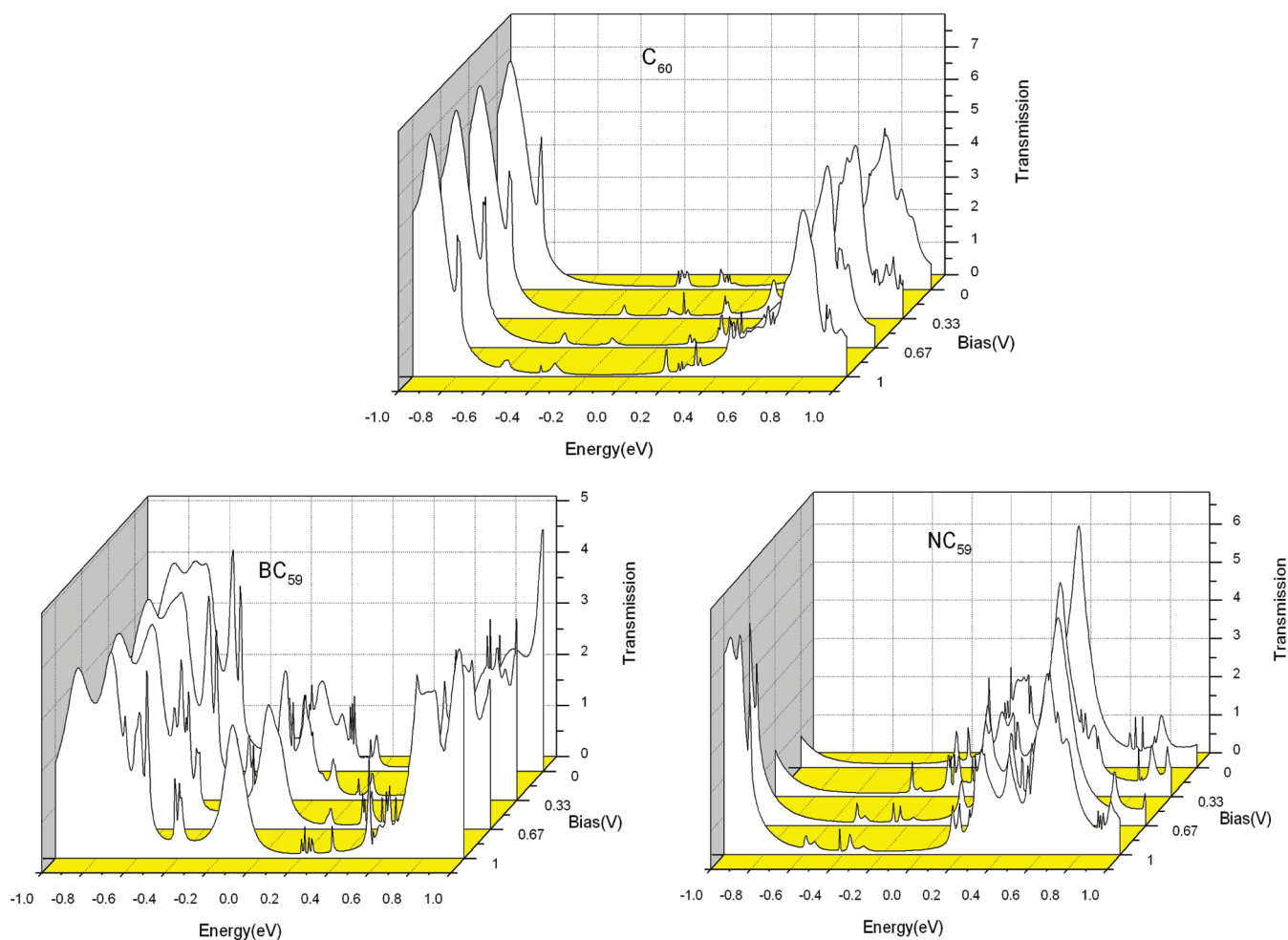


**Figure 3.** The bias-dependence of transmission functions of  $C_{60}$ ,  $BC_{59}$ , and  $NC_{59}$ . Zero of the energy is aligned to the Fermi energy.

easily at higher external bias. Thus, a hole-assisted electron transport mechanism in B-doped (*p*-type) fullerene appears to provide a higher electron conductivity. This suggests that fullerene can be an attractive candidate for *p*-type (B-doped) nanoelectronic devices.

The transport properties of substitutional fullerenes,  $BC_{59}$  and  $NC_{59}$ , were also studied previously.<sup>24</sup> The DFT-based calculations using the contact-fullerene distance of  $\sim 3.5$  Å find a nonlinear *I*–*V* characteristic for the doped fullerenes in the bias window of 0–1 V.<sup>50</sup> On the other hand, similar calculations<sup>24</sup> on  $BC_{59}$  and  $NC_{59}$  find that doping by B and N leads to a higher HOMO–LUMO gap and a smaller tunneling current with respect to that in the pristine fullerene. These findings are in stark contrast with the findings of the present study, which suggests the presence of midgap states associated with dopants in the HOMO–LUMO gap of  $C_{60}$ . It should be pointed out that the previous study<sup>24</sup> used asymmetric electrode architecture, considering three layers of Au (100) in the left lead and two layers of Au (100) in the right lead in the device architecture with the contact–fullerene distance to be 2.1 Å. Therefore, we suggest that the results of their calculations may be an artifact of the device model used in their calculations.

In an attempt to understand the effect of atomic level changes on the electronic structure and electron transport of molecular and nanoscale architecture, we have performed first-principles electronic structure calculations on  $C_{60}$  and its B- and N-doped derivatives. The cage structure of  $C_{60}$  allowed two different configurations, namely, endohedral ( $B@C_{60}$  and  $N@C_{60}$ ) and substitutional ( $BC_{59}$  and  $NC_{59}$ ), to be investigated. The calculated results clearly reveal that, at the nanoscale, even a single atom change in the structure brings about noticeable changes in the electronic and geometrical structures. Furthermore, the electron transport property of the nanoscale system gets substantially modulated by a single-atom change in the structure. Specifically, B and N doping of fullerene appears to lead to higher current than the pristine fullerene. However, the substitutional derivatives,  $BC_{59}$  and  $NC_{59}$ , in which the dopant atom occupies a site previously occupied by a C atom on the  $C_{60}$  wall, give higher magnitude of current than the endohedral derivatives,  $B@C_{60}$  and  $N@C_{60}$ . This is attributed to the dominance of hybrid states involving the contact gold atoms in forming the MOs near the Fermi region, which opens new transmission channels for the substitutional dopants. Finally, the calculations predict a much higher value of current for  $BC_{59}$  compared to all other species

considered here, suggesting its application as an effective *p*-type semiconductor in electronic devices.

## METHOD

The electron transport calculations were performed with the use of DFT together with the NEGF method. The current via a molecule can be obtained as

$$I = \frac{e}{h} \int_{-\infty}^{\infty} \det(E, V) [f(E - \mu_1) - f(E - \mu_2)] \quad (1)$$

where  $\mu_1$  and  $\mu_2$  are the electrochemical potentials in the two contacts under an external bias  $V$ , and  $f(E)$  is the Fermi–Dirac distribution function. The transmission function,  $T(E, V)$ , is an important intrinsic factor describing the quantum mechanical transmission probabilities for electrons. The semi-infinite effect of the left (right) electrode is taken into account by introducing the self-energy  $\Sigma_L$  ( $\Sigma_R$ ) in the effective Hamiltonian.<sup>25</sup> It is worth noting that the transmission depends on both the electron energy  $E$  and applied external bias  $V$ .

The local spin density approximation (LDA) of the exchange and correlation functional,<sup>26,27</sup> to DFT, incorporated in the SIESTA program package was used.<sup>28</sup> Double- $\zeta$  basis sets with polarization orbitals were used for all atoms. We used pseudopotentials for gold, which incorporates scalar relativistic corrections. The employed pseudopotentials are the standard in DFT calculations, and they describe the electronic structure of gold reasonably well. The bias-dependent electron transmission and current are calculated from the NEGF method based on the Keldysh formalism, as implemented in the SMEAGOL program.<sup>29,30</sup> A schematic illustration of the central scattering region of the model architecture is shown in Figure 1, where semi-infinite face-centered cubic gold contacts are represented by four  $6 \times 6 R$  gold bilayers along the (001) direction on either side of the contacts. In order to eliminate the interfacial effects introduced by thiol groups, generally used in quantum chemical calculations, gold atoms are directly bonded to  $C_{60}$ . The hexagonal faces of  $C_{60}$  are parallel to the gold contact layers with a separation distance of 2.4 Å. The gold atoms in the contact electrodes are fixed at the bulk value of a face-centered cubic structure, and the distance between the two (left and right) gold contact layers is  $\sim 11.9$  Å; the device architecture considered is just a parallel plate vacuum capacitor in the absence of  $C_{60}$ .

**SUPPORTING INFORMATION AVAILABLE** The details of the theoretical method, structural properties of pristine and doped fullerenes, density of states of doped and pristine  $C_{60}$ , and the bias-dependence of transmission functions of  $BC_{60}$  and  $NC_{60}$ . This material is available free of charge via the Internet at <http://pubs.acs.org>.

## AUTHOR INFORMATION

### Corresponding Author:

\*To whom correspondence should be addressed. E-mail: [pandey@mtu.edu](mailto:pandey@mtu.edu) (R.P.); [shashi.karna@us.army.mil](mailto:shashi.karna@us.army.mil) (S.P.K.).

**ACKNOWLEDGMENT** Helpful discussions with Haiying He and S. Gowtham are acknowledged. The work at Michigan Technological

University was performed under support by the Army Research Office through Contract Number W911NF-09-1-0221.

## REFERENCES

- (1) Nitzan, A.; Ratner, M. A. Electron Transport in Molecular Wire Junctions. *Science* **2003**, *300*, 1384.
- (2) He, H.; Pandey, R.; Karna, S. P. Electronic Conduction in a Model Three-Terminal Molecular Transistor. *Nanotechnology* **2008**, *19*, 505203.
- (3) Ravindran, S.; Chaudhary, S.; Colburn, B.; Ozkan, M.; Ozkan, C. S. Covalent Coupling of Quantum Dots to Multiwalled Carbon Nanotubes for Electronic Device Applications. *Nano Lett.* **2003**, *3*, 447–453.
- (4) Pasupathy, A. N.; Bialczak, R. C.; Martinek, J.; Grose, J. E.; Donev, L. A. K.; McEuen, P. L.; Ralph, D. C. The Kondo Effect in the Presence of Ferromagnetism. *Science* **2004**, *306*, 86–89.
- (5) He, H.; Pandey, R.; Karna, S. P. Electronic Structure Mechanism of Spin-Polarized Electron Transport in a Ni– $C_{60}$ –Ni System. *Chem. Phys. Lett.* **2007**, *439*, 110–114.
- (6) Joachim, C.; Gimzewski, J. K.; Schlittler, R. R.; Chavy, C. Electronic Transparency of a Single  $C_{60}$  Molecule. *Phys. Rev. Lett.* **1995**, *74*, 2102–2105.
- (7) Kroto, H. W.; Heath, J. R.; O'Brien, S. C.; Curl, R. F.; Smalley, R. E.  $C_{60}$ : Buckminster Fullerene. *Nature* **1985**, *318*, 162–163.
- (8) Oshiyama, A.; Saito, S.; Hamada, N.; Miyamoto, Y. Electronic Structures of  $C_{60}$  Fullerides and Related Materials. *J. Phys. Chem. Solids* **1992**, *53*, 1457–1471.
- (9) Zhao, J.; Zeng, C.; Cheng, X.; Wang, K.; Wang, G.; Yang, J.; Hou, J. G.; Zhu, Q. Single  $C_{59}N$  Molecule as a Molecular Rectifier. *Phys. Rev. Lett.* **2005**, *95*, 045502.
- (10) Zou, Y. J.; Zhang, X. W.; Li, Y. L.; Wang, B.; Yan, H.; Cui, J. Z.; Liu, L. M.; Da, D. A. Bonding Character of the Boron-Doped  $C_{60}$  Films Prepared by Radio Frequency Plasma Assisted Vapor Deposition. *J. Mater. Sci.* **2002**, *37*, 1043–1047.
- (11) Rockenbauer, A.; Csányi, G.; Fülöp, F.; Garaj, S.; Korecz, L.; Lukács, R.; Simon, F.; Forró, L.; Pekker, S.; Jánosy, A. Electron Delocalization and Dimerization in Solid  $C_{59}N$  Doped  $C_{60}$  Fullerene. *Phys. Rev. Lett.* **2005**, *94*, 066603.
- (12) Andreoni, W.; Gygi, F.; Parrinello, M. Impurity States in Doped Fullerenes:  $C_{59}B$  and  $C_{59}N$ . *Chem. Phys. Lett.* **1992**, *190*, 159–162.
- (13) Wang, S.-H.; Chen, F.; Fann, Y. C.; Kashani, M.; Malaty, M.; Jansen, S. A. Assessment of the Stability of Heterohedral Fullerenes: A Theoretical Analysis of  $C_{60-x}N_x$  and  $C_{60-x}B_x$  Where  $x = 1$  and  $2$ . *J. Phys. Chem.* **1995**, *99*, 6801–6807.
- (14) Andreoni, W.; Curioni, A.; Holczer, K.; Prassides, K.; Keshavarz-K, M.; Hummelen, J.-C.; Wudl, F. Unconventional Bonding of Azafullerenes: Theory and Experiment. *J. Am. Chem. Soc.* **1996**, *118*, 11335–11336.
- (15) Saunders, M.; Jiménez-Vázquez, H. A.; Cross, R. J.; Poreda, R. J. Stable Compounds of Helium and Neon:  $He@C_{60}$  and  $Ne@C_{60}$ . *Science* **1993**, *259*, 1428–1430.
- (16) Shinohara, H. Endohedral Metallofullerenes. *Rep. Prog. Phys.* **2000**, *63*, 843–892.
- (17) Barajas-Barraza, R. E.; Guirado-Lopez, R. A. Endohedral Nitrogen Storage in Carbon Fullerene Structures: Physisorption to Chemisorption Transition with Increasing Gas Pressure. *J. Chem. Phys.* **2009**, *130*, 234706–234709.
- (18) Feyereisen, M.; Gutowski, M.; Simons, J.; Almlof, J. Relative Stabilities of Fullerene, Cumulene, and Polyacetylene Structures for  $C_n$ :  $n = 18–60$ . *J. Chem. Phys.* **1992**, *96*, 2926–2932.

- (19) Lin, F.; Sørensen, E. S.; Kallin, C.; Berlinsky, A. J. Single-Particle Excitation Spectra of C<sub>60</sub> Molecules and Monolayers. *Phys. Rev. B* **2007**, *75*, 075112.
- (20) Park, H.; Park, J.; Lim, A. K. L.; Anderson, E. H.; Alivisatos, A. P.; McEuen, P. L. Nanomechanical Oscillations in a Single-C<sub>60</sub> Transistor. *Nature* **2000**, *407*, 57–60.
- (21) Nakanishi, S.; Tsukada, M. Quantum Loop Current in a C<sub>60</sub> Molecular Bridge. *Phys. Rev. Lett.* **2001**, *87*, 126801.
- (22) Taylor, J.; Guo, H.; Wang, J. Ab Initio Modeling of Open Systems: Charge Transfer, Electron Conduction, and Molecular Switching of a C<sub>60</sub> Device. *Phys. Rev. B* **2001**, *63*, 121104.
- (23) Lau, K. C.; Pandey, R.; Pati, R.; Karna, S. P. Theoretical Study of Electron Transport in Boron Nanotubes. *Appl. Phys. Lett.* **2006**, *88*, 212111–212113.
- (24) Zhang, X.-J.; Long, M.-Q.; Chen, K.-Q.; Shuai, Z.; Wan, Q.; Zou, B. S.; Zhang, Y. Electronic Transport Properties in Doped C<sub>60</sub> Molecular Devices. *Appl. Phys. Lett.* **2009**, *94*, 073503–073503.
- (25) Datta, S. *Electronic Transport in Mesoscopic Systems*; Cambridge University Press: Cambridge, U.K., 1995.
- (26) Ceperley, D. M.; Alder, B. J. Ground State of the Electron Gas by a Stochastic Method. *Phys. Rev. Lett.* **1980**, *45*, 566–569.
- (27) Perdew, J. P.; Zunger, A. Self-Interaction Correction to Density-Functional Approximations for Many-Electron Systems. *Phys. Rev. B* **1981**, *23*, 5048–5079.
- (28) Soler, J. M.; Artacho, E.; Gale, J. D.; García, A.; Junquera, J.; Ordejón, P.; Sánchez-Portal, D. The SIESTA Method for Ab Initio Order-N Materials Simulation. *J. Phys.: Condens. Matter* **2002**, *14*, 2745.
- (29) Rocha, A. R.; García-Suárez, V. M.; Bailey, S. W.; Lambert, C. J.; Ferrer, J.; Sanvito, S. Computer Code SMEAGOL: Spin and Molecular Electronics in Atomically Generated Orbital Landscapes. *Phys. Rev. B* *73*, 085414, **2006** (see also, <http://www.smeagol.tcd.ie/>).
- (30) Rocha, A. R.; Garcia-suarez, V. M.; Bailey, S. W.; Lambert, C. J.; Ferrer, J.; Sanvito, S. Towards Molecular Spintronics. *Nat. Mater.* **2005**, *4*, 335–339.